Available online at www.sciencedirect.com
ScienceDirect
Journal of the European Ceramic Society 28 (2008) 611–616
www.elsevier.com/locate/jeurceramsoc

Glass and composite seals for the joining of YSZ to metallic interconnect in solid oxide fuel cells

F. Smeacetto [a,*], M. Salvo [a], M. Ferraris [a], V. Casalegno [a], P. Asinari [b]

[a] *Materials Science and Chemical Engineering Department, Politecnico di Torino, C.so Duca degli Abruzzi 24, 10129 Torino, Italy*
[b] *Department of Energetics, Politecnico di Torino, C.so Duca degli Abruzzi 24, 10129 Torino, Italy*

Received 28 September 2006; received in revised form 5 July 2007; accepted 14 July 2007
Available online 14 September 2007

Abstract

This paper describes the design and development of a composite seal for SOFC to produce a hermetic joint between the ceramic and metallic components of the SOFC stacks. The composite seal was designed to be chemical compatible with the ceramic electrolyte (YSZ) and the interconnect (AISI 430), to have suitable thermo-mechanical properties (T_g, thermal expansion coefficient, TEC), and good wettability with them. The reinforcing phase (alumina) was chosen to increase the seal viscosity at the SOFC working temperature (about 800 °C), to improve the thermal shock resistance of the seal and to match the thermal expansion coefficient of the components to be joined.

The seal was morphological and thermo-mechanical characterized by scanning electron microscopy, SEM, energy dispersive spectroscopy, EDS, thermo-mechanical analysis, TMA, X-ray diffraction, XRD and differential thermal analysis, DTA.

The joining process between YSZ and AISI 430 was optimized taking into account that the maximum process temperature should be around 1000 °C. Joined samples were preliminary submitted to H_2–3% H_2O atmosphere exposure at 800 °C for 200 h.

Keywords: Joining; Interfaces; Glass; Fuel cells; YSZ

1. Introduction

Fuel cells convert chemical energy into electrical energy with high efficiency and low emission of pollutants.[1] Among the different SOFCs, the planar type, which is expected to be cost effective and mechanically robust, offers an attractive potential for the increased power densities compared to other fuel cell concepts. The repeating unit of a planar configuration is formed by anode–electrolyte–cathode and interconnect; the interconnect provides electrical connection between the anode of one individual cell (repeating unit) to the cathode of the neighboring one. In most planar solid oxide fuel cell stack designs, the interconnect has to be sealed to the adjacent ceramic components; as interconnect, chromia-forming ferritic stainless steels are among the most promising candidates, due to their electrically conducting oxide scale,[2] appropriate thermal expansion behavior, and low cost. The seal has to meet some important requirements: it should be hermetic, in order to prevent mixing of fuel and oxidant; it should match its thermal expansion coefficient to the interconnect and anode–cathode–electrolyte ones, depending on stack design; it must provide electrical isolation of the cell and a low reactivity with the other cell components over the lifetime of the cell, when in contact with both the fuel and the air sides of the electrolyte.

Different seal concepts have been proposed: rigid glass or glass-ceramic seals,[3–7] glass-ceramic composite seals[8] or compressive seals such as micas.[9–11]

A glass- or a glass-ceramic matrix composite seal should have several advantages[12]: e.g., the thermo-mechanical properties of the composite seal (viscosity, thermal expansion coefficient, thermal conductivity) can be controlled by volume fraction and particle size of the second phase, the glass matrix can flow to mitigate stresses and to heal cracks and the conversion of the glass in a more stable glass-ceramic can improve the mechanical properties of the seal.[13–16]

In this study, two sodium–calcium–aluminosilicate glasses (SACN1 and SACN2) were developed as glassy seals and as matrix for glass-ceramic composite seals for joining components

* Corresponding author. Tel.: +39 011564706; fax: +39 0115644699.
E-mail address: federico.smeacetto@polito.it (F. Smeacetto).

0955-2219/$ – see front matter © 2007 Elsevier Ltd. All rights reserved.
doi:10.1016/j.jeurceramsoc.2007.07.008

in SOFC planar configuration. The sealing materials were produced in an amorphous state; the subsequent introduction of a second phase and the thermal treatment for joining AISI 430 and YSZ determined the formation of a glass-ceramic matrix composite seal.

The sealing materials were barium oxide free, in order to avoid the formation of high thermal expansion coefficient barium chromate, due to the interaction with chromium oxide on the surface of AISI 430.[17]

The second phase, Al_2O_3 particles, was chosen to increase the seal viscosity at the SOFC working temperature (about 800 °C) and to improve the thermal shock resistance of the seal. In fact, the most critical aspect of the known seals is their low resistance to thermal cycling for prolonged time: the mechanical strength improvement and the higher thermal conductivity, which can be obtained by using alumina as reinforcing phase, should increase the thermal fatigue resistance of the seal.

2. Experimental

The heat resistant metal alloy used for this study was AISI 430, a ferritic stainless steel containing 16 wt.% of chromium (thermal expansion coefficient: $11.5 \times 10^{-6}\,K^{-1}$). For the wettability experiments, AISI 430 plates (15 mm × 10 mm × 2 mm) were ultrasonic cleaned in acetone, then used as as-received or pre-oxidized in air (900 °C, 2 h).

The 8% mol yttria stabilized zirconia wafers (15 mm × 10 mm × 1 mm), with a thermal expansion coefficient of $10.5 \times 10^{-6}\,K^{-1}$, were supplied by InDec Ltd. (The Netherlands).

The two glasses, labeled as SACN1 and SACN2, were produced by melting the raw materials (SiO_2, Al_2O_3, Na_2CO_3, $CaCO_3$ and H_3BO_3) at 1500 °C for 1 h in a platinum crucible; the glasses were poured on a brass plate and subsequently powdered (40–68 μm). The molar compositions of the two glasses are—SACN1: SiO_2 (45%), Al_2O_3 (9%), CaO (18%), Na_2O (18%) and B_2O_3 (10%); SACN2: SiO_2 (40%), Al_2O_3 (9%), CaO (18%), Na_2O (23%) and B_2O_3 (10%). Their thermal expansion coefficients were measured on glass bars (8 mm × 5 mm × 4 mm) in a Perkin–Elmer DMA, (heating rate 5 °C/min). The glass transition temperatures were measured by DSC (Perkin–Elmer DSC 7) and DTA (Perkin Elmer DTA 7).

The wettability of both glasses on AISI 430 and YSZ was studied by heating stage microscopy (LEITZ Wetzlar, Germany) in air and under Ar flow. The joined samples were processed according to the set-up shown in Fig. 1. The AISI 430/seal/YSZ samples were prepared by slurry technique, i.e., dispersion of glass powders in ethanol; the slurry was deposited at room temperature between the pre-oxidized AISI 430 plate and the YSZ wafer, then heat treated in a tubular oven, under Ar atmosphere, at temperature above glass softening point, i.e., from room temperature to 1000 °C with a dwelling time of 30 min at 1000 °C, heating rate of 20 °C/min.

Fig. 1. Schematic view of the joint between YSZ and AISI 430.

In order to obtain the AISI 430/composite seal/YSZ, the procedure was the same as described above, but alumina particles were added (10–20 vol.%, 20 μm particle average diameter) and mixed to the SACN slurry, In this case, the joining thermal treatment was from room temperature to 1020 °C (dwelling time 30 min, under Ar flow).

Polished cross-sections of the joined specimens were examined by scanning electron microscopy (SEM, Jeol) and optical microscopy.

Crystalline phases formed in the composite seal were detected by XRD diffraction.

Both AISI 430/seal/YSZ and AISI 430/composite seal/YSZ joined samples were submitted to H_2–3% H_2O atmosphere exposure at 800 °C for 200 h. Reducing conditions were obtained by using H_2 gas, which was humidified by passing over a water bath at 22.8 °C.

Polished cross-sections of the tested specimens were examined by scanning electron microscopy (SEM, Jeol) equipped with EDS.

3. Results and discussion

3.1. Wetting and adhesion

SACN2 glass has a higher amount of sodium than SACN1 (see Section 2 details); the consequence is a higher thermal expansion coefficient and also a lower viscosity, as it can be observed in Table 1 (where the characteristic temperatures and TECs for the two glasses are summarized); as a consequence SACN2 could be deposited at lower temperatures than SACN1.

Fig. 2 shows a comparison among the coefficients of thermal expansion of the AISI 430, the YSZ and the two glasses (SACN1 and SACN2); it can be observed that SACN2 TEC has an intermediate value between the AISI 430 and the YSZ.

The wettability tests of glasses on AISI 430 (as received and pre-oxidized) and on YSZ plates were conducted at different temperatures (1040 °C for SACN1 and 1000 °C for SACN2) in air or argon atmosphere. The AISI 430 substrates were pre-oxidized with the aim of forming an adherent oxide layer compatible with both glass and metal substrate, whose function was to act as transition layer and to promote strong chemical bonding between metal and seal.[18] The pre-oxidation gave rise to the formation of a 3–5 μm thick chromium–manganese

Table 1
Characteristic temperatures and TECs for the SACN1 and SACN2

	T_g (°C) (DSC)	T_s (heating microscope) (°C)	Thermal expansion coefficient ($\times 10^{-6}$ °C^{-1}) (200–400 °C)
SACN1	580	740	9.3
SACN2	545	680	11.2

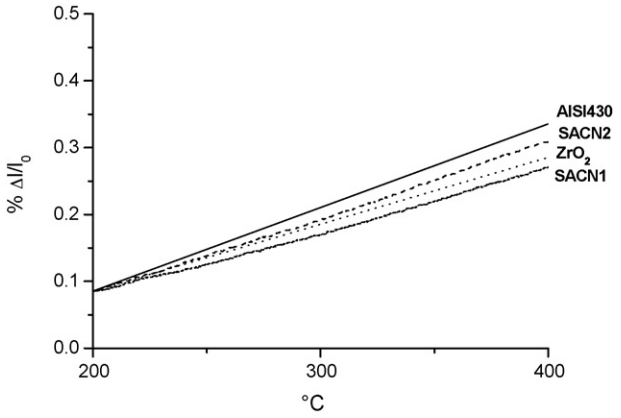

Fig. 2. Thermal expansion coefficients of; the AISI 430, YSZ and the two glasses (SACN1 and SACN2).

oxide and chromium–iron oxide layer, as detected by XRD and SEM.

Table 2 summarizes observations on wetting and adhesion tests: the two glasses showed good wettability on both substrates, but in many cases seal/AISI 430 interfaces detached during cooling from test temperature; the best results (crack-free and continuous interface, no pores into the glass seal) were obtained using SACN2 on the pre-oxidized AISI 430, under argon flow. Then, the production of a pre-oxidation layer on AISI 430 was really effective to increase the interface bonding between metal and seal, but it was not sufficient with high thermal expansion coefficient mismatches (i.e., SACN1/AISI 430 samples).

In fact, the lower value of the SACN1 TEC results in a low quality and somewhere detached interface between the glass matrix and the pre-oxidized AISI 430; besides, some cracks are present near the SACN1 glass/AISI 430 interface (Fig. 3).

The interfacial adhesion of SACN2, whose TEC is very closed to AISI 430, with pre-oxidized AISI 430 was clearly better, as it can be observed in Fig. 4, where no cracks or pores are present. A partial infiltration of the glass is visible through the chromium–iron manganese oxides rich layer; no bubbles or cracks are present in the glass joint. As a consequence of these results, the SACN2 glass was chosen as seal and as a matrix for the composite seal.

3.2. Seal processing and characterization

3.2.1. Glass seal

The joining between the pre-oxidized AISI 430 and the YSZ plate by SACN2 glass was carried out by heating in argon atmosphere up to 1000 °C for 30 min chosen as the best experimental conditions in terms of interface morphology.

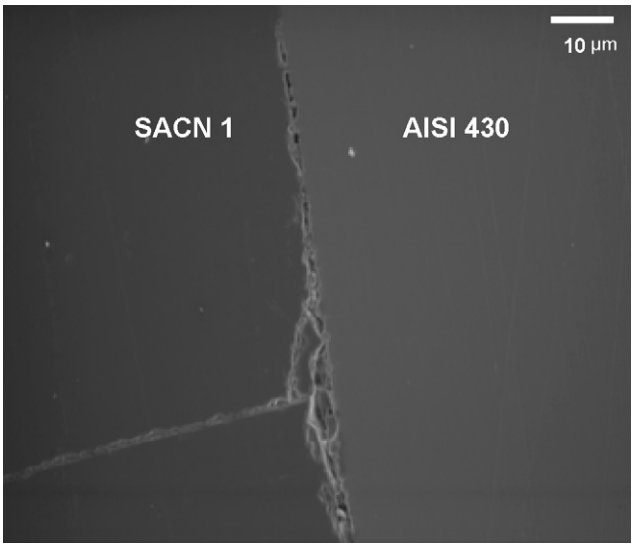

Fig. 3. SEM micrograph: cross-section of the interface between pre-oxidized AISI 430 and SACN1 (1040 °C, 30 min).

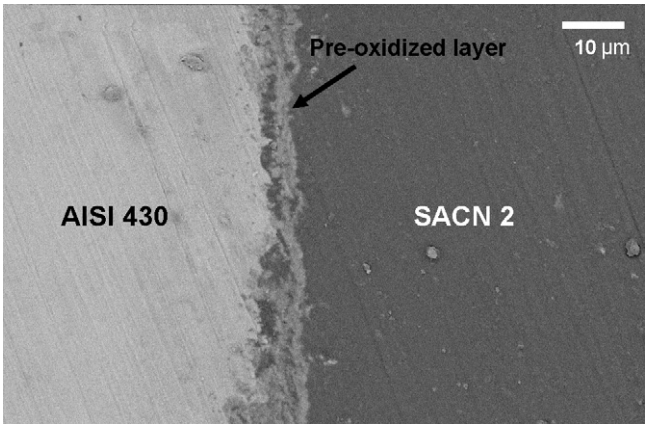

Fig. 4. SEM micrograph: cross-section of the interface between pre-oxidized AISI 430 and SACN2 glass (1000 °C, 30 min).

Fig. 5 is a SEM micrograph of the cross-section of the joined AISI 430/SACN2/YSZ sample; the average thickness of the joint is 300 μm. The absence of cracks near the interface both with AISI 430 and YSZ demonstrates the good matching of SACN2 TEC with both the substrates to be joined (in Fig. 2, SACN2 TEC is intermediate between AISI 430 and YSZ); the SACN2 glass joint region is free from pores and cracks perpendicular

Table 2
Wetting and adhesion experimental observations for SACN1 and SACN2 on AISI 430 and YSZ

	AISI 430 (under Ar flow)	AISI 430 (air)	Pre-oxidized-AISI 430	YSZ (air)
SACN1 (1040 °C)	Completely detached	Partially detached pores at interface	Partially detached, cracks	Good wetting, good interface
SACN2 (1000 °C)	Completely detached	Partially detached	Good wetting, good interface, no cracks	Good wetting, good interface, no cracks
Composite seal (1020 °C)	–	–	Good wetting, good interface, no cracks	Good wetting, good interface, no cracks

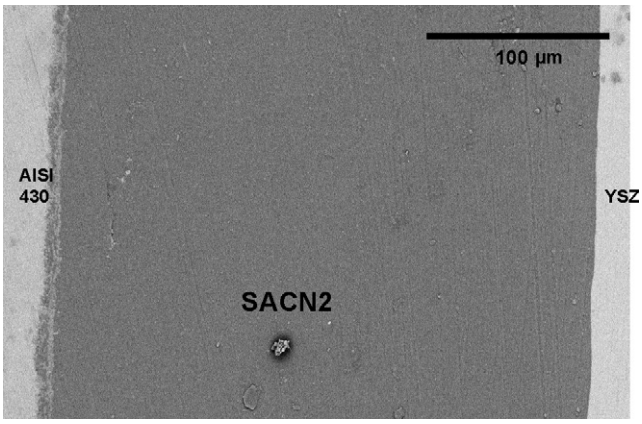

Fig. 5. SEM micrograph of the cross-section of the joint AISI 430/SACN2/YSZ (1000 °C, 30 min).

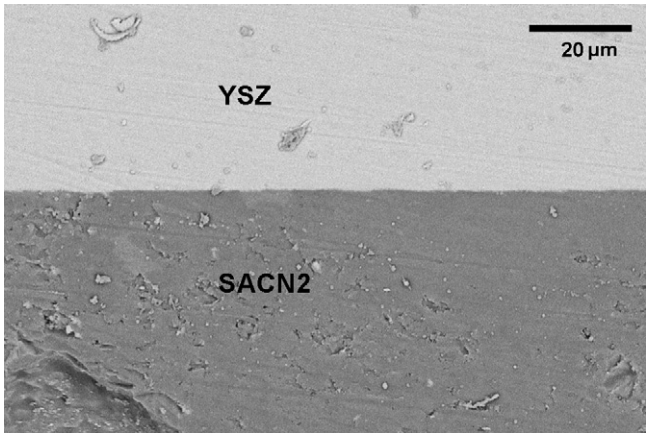

Fig. 6. SEM micrograph: magnification of the interface between the SACN2 and YSZ (1000 °C, 30 min).

to the substrate surfaces; no morphological evidence of precipitates or crystalline phases was found in the SACN2 joint region.

Fig. 6 is a magnification of the interface zone between the SACN2 and the YSZ plate; the interface is continuous and without pores or cracks.

3.2.2. Glass-ceramic matrix composite seal

The SOFC working temperature should be around 800 °C for several hours; the main advantages of the composite seal, compared to the glass seal, are the enhanced toughness, thermal chock resistance and viscosity. In particular, enhanced viscosity of the composite seal should avoid the sealant flow at the working temperature, still assuring the healing of cracks at working condition.

The composite joint between pre-oxidized AISI 430 and the YSZ plate, with the SACN2 added with 10–20 vol.% alumina particles, was obtained at temperature of 1020 °C, for 30 min in argon atmosphere: this process caused the crystallization of the SACN2 glass matrix, as can be observed by the X-ray diffraction pattern of Fig. 7; the detected crystalline phases are $Ca_2Al_2SiO_7$, $AlNa(SiO_4)$ and residual aluminum oxide.

The estimated TEC of the composite seal $10.84 \times 10^{-6}\,K^{-1}$, calculated according to the rule of mixtures, is intermediate between AISI 430 and YSZ.

Fig. 8 shows an optical micrograph of the interface between pre-oxidized AISI 430 and composite seal: the experimental evidence was the absence of cracks in the joint region; a good dispersion of alumina particles in the SACN2 matrix was achieved. SEM observation of the cross-section (picture not reported here) of the joint AISI 430/SACN2/YSZ, showed the absence of cracks in the joint region; anyway a residual porosity was present in the joint region, probably due to the high viscosity of the composite seal and to its shrinkage during crystallization.

Finally, an EDS analysis (see Fig. 9) on the composite seal up to 20 μm from the interface with the pre-oxidized AISI 430 substrate did not detect any Cr-diffusion.

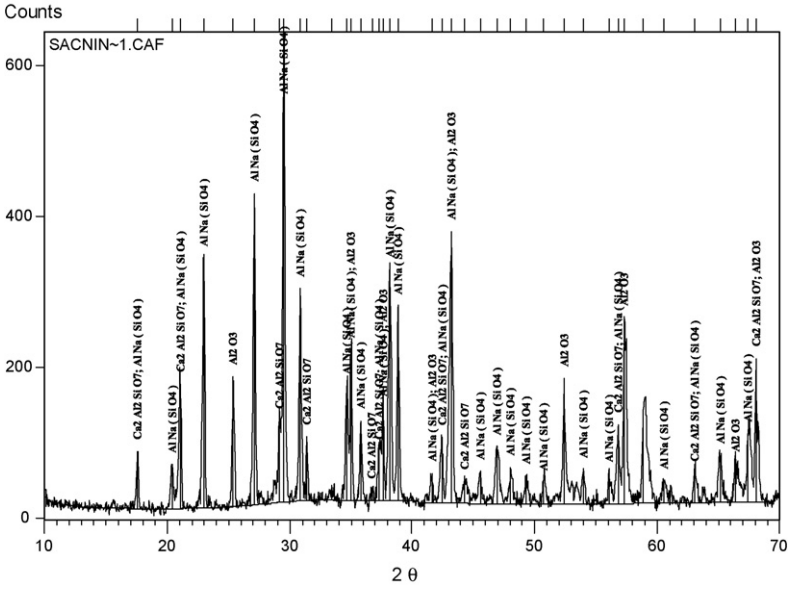

Fig. 7. X-ray diffraction pattern of the composite seal.

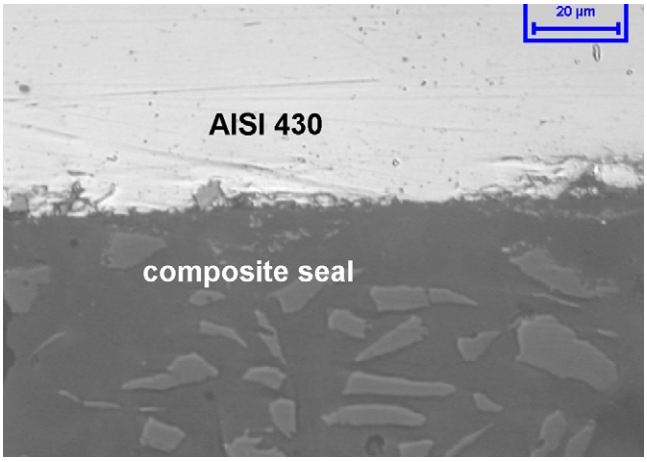

Fig. 8. Optical micrograph of the interface between pre-oxidized AISI 430 and the composite seal (1020 °C, 30 min).

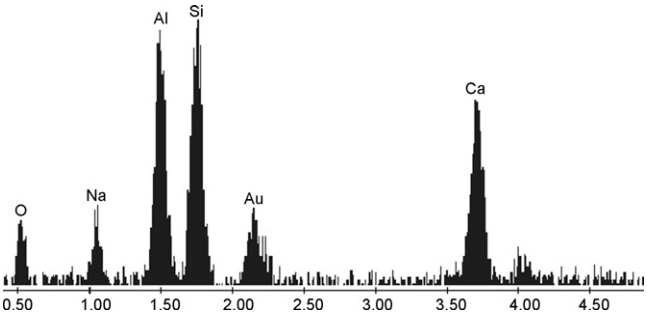

Fig. 9. EDS analysis on the composite seal up to 20 µm from the interface with the pre-oxidized AISI 430.

3.2.3. *Exposure of the joined samples to H_2–3% H_2O atmosphere*

Both AISI 430/seal/YSZ and AISI 430/composite seal/YSZ joined samples were submitted to H_2–3% H_2O atmosphere exposure at 800 °C for 200 h.

In the case of glassy seal, a high degree of corrosion was observed both in the joint region and in the metallic interconnect at the three-phase boundary. Fig. 10 shows the three-phase boundary for AISI 430/seal samples; a severe degree of corrosion was observed, together with a high amount of chromium, iron and manganese oxides diffusion into the seal. EDS analysis conducted on a point at 20 µm from AISI/seal interface, revealed the presence of oxygen, chromium, manganese and iron.

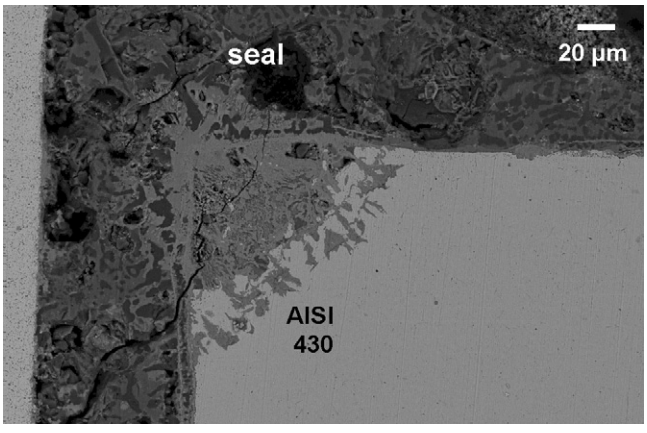

Fig. 10. Three-phase boundary for AISI 430/seal sample, after exposure for 200 h at 800 °C to H_2–3% H_2O atmosphere.

More promising results were obtained after the test on samples joined by the composite seal. Fig. 11a shows the cross-section of AISI 430/composite seal/YSZ joined sample after exposure for 200 h at 800 °C to H_2–3% H_2O atmosphere. No presence of cracks was observed and the AISI 430/composite seal and composite seal/YSZ interfaces are still continuous and flawless. A slight interface corrosion is confined to the AISI 430/composite seal three-phase boundary (Fig. 11b), where the thickness of the chromium, iron, manganese oxide layer increased to about 10 µm.

The mechanism for corrosion at the three-phase boundary is due to the decomposition of sodium oxide under reducing conditions, as described in Ref. 19.

The difference in corrosion behavior between AISI 430/seal/YSZ and AISI 430/composite seal/YSZ joined samples at the three-phase boundary was probably due to the higher viscosity of the composite seal together with the higher thermodynamic stability of glass-ceramic composite structure (where $Ca_2Al_2SiO_7$, $AlNa(SiO_4)$ crystalline phases were formed) with respect to the glassy seal.

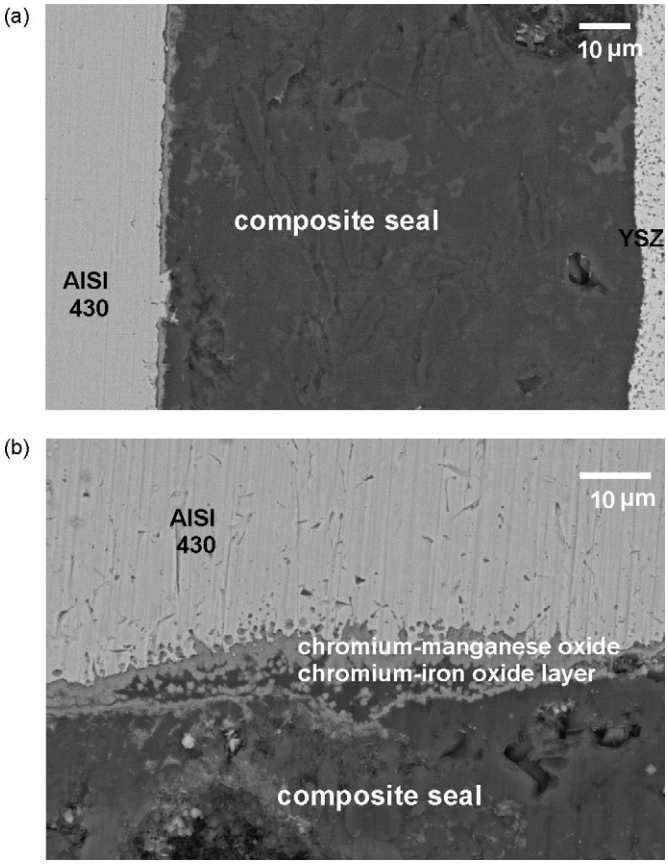

Fig. 11. (a) Cross-section of AISI 430/composite seal/YSZ joined sample after exposure for 200 h at 800 °C to H_2–3% H_2O atmosphere. (b) Three-phase boundary for AISI 430/composite seal, after exposure for 200 h at 800 °C to H_2–3% H_2O atmosphere.

Anyway, the AISI 430 corrosion and consequently the reactivity at the AISI 430/seal interface region, could be further reduced by application of thin more stable metal-oxide coating to the AISI 430 interconnect, prior to sealing.[19]

4. Conclusions

A new barium-free multi-component borosilicate glass has been successfully used to seal AISI 430 to YSZ.

A composite seal based on this glass showed a good interface with pre-oxidized AISI 430 and the YSZ; no reactions were observed at the deposition temperatures, but a residual porosity is still present in the composite seal. Joined samples were preliminary submitted to H_2–3% H_2O atmosphere exposure at 800 °C for 200 h. The morphological analysis showed integrity of the AISI 430/composite seal/YSZ joint region, but at the three-phase boundary a slight corrosion zone were observed.

References

1. Steele, B. C. H. and Heinzel, A., Materials for fuel-cell technologies. *Nature*, 2001, **414**, 345–352.
2. Zhu, W. Z. and Deevi, S. C., Development of interconnect materials for solid oxide fuel cells. *Materials Science and Engineering A*, 2003, **348**, 227–243.
3. Yang, Z., Xia, G., Meinhardt, K. D., Weil, K. S. and Stevenson, J. W., Chemical stability of glass seal interfaces in intermediate temperature solid oxide fuel cells. *Journal of Materials Engineering and Performance*, 2004, **13**, 327–334.
4. Nielsen, K. A., Solvang, M., Poulsen, F. W. and Larsen, P. H., Evaluation of sodium aluminosilicate glass composite seal with magnesia filler. In *Proceedings of the Ceramic Engineering and Science 25*, 2004, pp. 309–314.
5. Meinhardt, *et al.*, Glass-ceramic joint and method of joining, US Patent 6,532,769 B1, March 18, 2003.
6. Yang, Z., Stevenson, J. W. and Meinhardt, K. D., Chemical interactions of barium–calcium–aluminosilicate-based sealing glasses with oxidation resistant alloys. *Solid State Ionics*, 2003, **160**, 213–225.
7. Sohn, S. B., Choi, Se.-Y., Kim, G.-H., Song, H.-S. and Kim, G.-D., Stable sealing glass for planar solid oxide fuel cell. *Journal of Non Crystalline Solids*, 2002, **297**, 103–112.
8. Xue, *et al.*, Composite sealant materials for solid oxide fuel cells, US Patent 6,271,158 B1, August 7, 2001.
9. Chou, Y. S. and Stevenson, J. W., Phlogopite mica-based compressive seals for solid oxide fuel cells: effect of mica thickness. *Journal of Power Sources*, 2003, **124**(2), 473–478.
10. Chou, Y. S. and Stevenson, J. W., Mid-term stability of novel mica-based compressive seals for solid oxide fuel cells. *Journal of Power Sources*, 2003, **115**(2), 274–278.
11. Chou, Y. S. and Stevenson, J. W., Thermal cycling and degradation mechanism of compressive mica-based seals for solid oxide fuel cells. *Journal of Power Sources*, 2002, **112**(2), 376–383.
12. Loehman, R., Dumm, H. P. and Hofer, H., Evaluation of sealing glasses for solid oxide fuel cells. In *Proceedings of the Ceramic Engineering and Science 23*, 2002, pp. 699–710.
13. Sohn, S.-B., Choi, S.-Y., Kim, G.-H., Song, H.-S. and Kim, G.-D., Suitable Glass-ceramic sealant for planar solid-oxide fuel cells. *Journal of the American Ceramic Society*, 2004, **87**, 254–260.
14. Fergus, J. W., Sealants for solid oxide fuel cells. *Journal of Power Sources*, 2005, **147**, 46–57.
15. Bansal, N. P. and Gamble, E. A., Crystallization kinetics of a solid oxide fuel cell seal glass by differential thermal analysis. *Journal of Power Sources*, 2005, **147**, 107–115.
16. Brochu, M., Gauntt, B. D., Shah, R., Miyake, G. and Loehman, R. E., Comparison between barium and strontium-glass composites for sealing SOFCs. *Journal of the European Ceramic Society*, 2006, **26**, 3307–3313.
17. Yang, Z., Weil, K. S., Paxton, D. M. and Stevenson, J. W., Selection and evaluation of heat-resistant alloys for SOFC interconnect applications. *Journal of The Electrochemical Society*, 2003, **150**(9), A1188–A1201.
18. Hong, F. and Holland, D., Studies of interface reactions between glass ceramic coatings and metals. *Journal of Non Crystalline Solids*, 1989, **112**, 357–363.
19. Nielsen, K. A., Solvang, M., Nielsen, S. B. L., Dinesen, A. R., Beeaff, D. and Larsen, P. H., Glass composite seal for SOFC application. *Journal of the European Ceramic Society*, 2007, **27**, 1817–1822.